Earth and Planetary Science Letters 281 (2009) 134–146

Contents lists available at ScienceDirect

Earth and Planetary Science Letters

journal homepage: www.elsevier.com/locate/epsl

Unsteady evolution of the Bolivian Subandean thrust belt: The role of enhanced erosion and clastic wedge progradation

Cornelius E. Uba [a,*], Jonas Kley [b], Manfred R. Strecker [a], Axel K. Schmitt [c]

[a] Institut für Geowissenschaften, Universität Potsdam, Karl-Liebknechtstr. 24, 14476 Potsdam, Germany
[b] Institut für Geowissenschaften, Universität Jena, Burgweg 11, 07749 Jena, Germany
[c] Department of Earth and Space Sciences, University of Los Angeles, California, USA

ARTICLE INFO

Article history:
Received 18 July 2008
Received in revised form 11 December 2008
Accepted 6 February 2009
Available online 25 March 2009

Editor: T.M. Harrison

Keywords:
Central Andes
deposition pinch-out migration
thrust belt propagation rates
orogenic wedge
climate
erosion

ABSTRACT

The Subandean fold and thrust belt of Bolivia constitutes the easternmost part of the Andean orogen that reflects thin-skinned shortening and eastward propagation of the Andean deformation front. The exact interplay of tectonics, climate, and erosion in the deposition of up to 7.5 km of late Cenozoic strata exposed in the Subandes remains unclear. To better constrain these relationships, we use four W–E industry seismic reflection profiles, eight new zircon U–Pb ages from Mio-Pliocene sedimentary strata, and cross-section balancing to evaluate the rates of thrust propagation, shortening, and deposition pinch-out migration. Eastward thrusting arrived in the Subandean belt at ~12.4±0.5 Ma and propagated rapidly toward the foreland unit approximately 6 Ma. This was followed by out-of-sequence deformation from ca. 4 to 2.1 Ma and by renewed eastward propagation thereafter. Our results show that the thrust-front propagation- and deposition pinch-out migration rates mimic the sediment accumulation rate. The rates of deposition pinch-out migration and thrust propagation increased three- and two fold, respectively (8 mm/a; 3.3 mm/a) at 8–6 Ma. The three-fold increase in deposition pinch-out migration rate at this time is an indication of enhanced erosional efficiency in the hinterland, probably coupled with flexural rebound of the basin. Following the pulse of pinch-out migration, the Subandean belt witnessed rapid ~80 km eastward propagation of thrusting to the La Vertiente structure at 6 Ma. As there is no evidence for this event of thrust front migration being linked to an increase in shortening rate, the enhanced frontal accretion suggests a shift to supercritical wedge taper conditions. We propose that the supercritical state was due to a drop in basal strength, caused by sediment loading and pore fluid overpressure. This scenario implies that climate-controlled variation in erosional efficiency was the driver of late Miocene mass redistribution, which induced flexural rebound of the Subandean thrust belt, spreading of a large clastic wedge across the basin, and subsequent thrust-front propagation.

1. Introduction

The Subandean fold-and-thrust belt of the Central Andes is the type-example of an active thin-skinned fold-and-thrust belt in a retroarc, non-collisional tectonic setting (e.g., Gubbels et al., 1993; Dunn et al., 1995; Kley et al., 1996; Moretti et al., 1996; Echavarria et al., 2003). With a maximum elevation of 1.7 km, this tectonic province is located to the east of the Cordillera Oriental and the Altiplano in the orogen interior. The Subandes are characterized by NNE–SSW oriented thrusting and deeply incised valleys that are connected with the foreland. Many investigations have ascribed shallow crustal shortening in this region directly to the crustal thickening processes that produced the Altiplano (e.g., Isacks, 1988; Gubbels et al., 1993).

The chronology of the clastic sediments preserved within and adjacent to the Subandes furnishes a unique archive about the geodynamic, topographic, and climatic evolution of the Andean tectonic provinces. Furthermore, volcanic ash horizons in the thick synorogenic Subandean strata of Bolivia provide the opportunity to develop a chronology of deformation and depositional processes and to study the interaction between tectonics, climate, and erosion.

To date the study by Echavarria et al. (2003) provides the only well-constrained study concerning the geometry and timing of the Subandean fold-and-thrust-belt in adjacent northwestern Argentina, documenting lowered shortening rate of 0–5 mm/yr between 7 and 2 Ma. In the central Andes, Garzione et al. (2006) and Ghosh et al. (2006) used oxygen isotope data obtained from paleosol carbonates to propose that the northern Altiplano rose to an elevation of ~3900 m between 10.3 and 6.8 as a result of mantle delamination. However, the lack of quantitative data for most of the Subandean region, especially in the north and east of these investigations, has hampered the validation of these models. Surprisingly, despite the fundamental role

* Corresponding author.
E-mail address: uba@geo.uni-potsdam.de (C.E. Uba).

0012-821X/$ – see front matter © 2009 Elsevier B.V. All rights reserved.
doi:10.1016/j.epsl.2009.02.010

attributed to the Subandean belt in conjunction with the evolution of the orogen interior, relatively little is known about the timing and magnitude of deformation in the Subandes. Indeed, a rigorous assessment of timing of deformation, propagation rate of the thrust belt, and the relationship between tectonics and climate-driven processes in shaping the Subandes has been prevented by the lack of a reliable chronostratigraphy and rigorous analyses of the Neogene synorogenic stratigraphic records.

With this study, we aim to unravel and better constrain the onset of thrusting, propagation of deformation, and erosional processes in the Bolivian Subandes. To achieve this, we used 8 new zircon U–Pb age determinations augmented by recently published ages across the belt (Echavarria et al., 2003; Hulka, 2005; Uba et al., 2007), industry seismic reflection profiles, well-log data, and outcrop studies. Our new chronology combined with deposition pinch-out migration and sedimentologic data provides a detailed record of the tectonic evolution of the Subandes in Bolivia. In addition, this study furnishes proxies for past erosional and transport efficiency, and information on the mechanisms governing deformation patterns in this thrust belt.

2. Geological setting and late Cenozoic stratigraphy of the Subandean zone

The central Andean evolution is linked to subduction of the Farallon/Nazca plate under the South American plate. In the course of the non-collisional mountain building in the Andes, under-thrusting

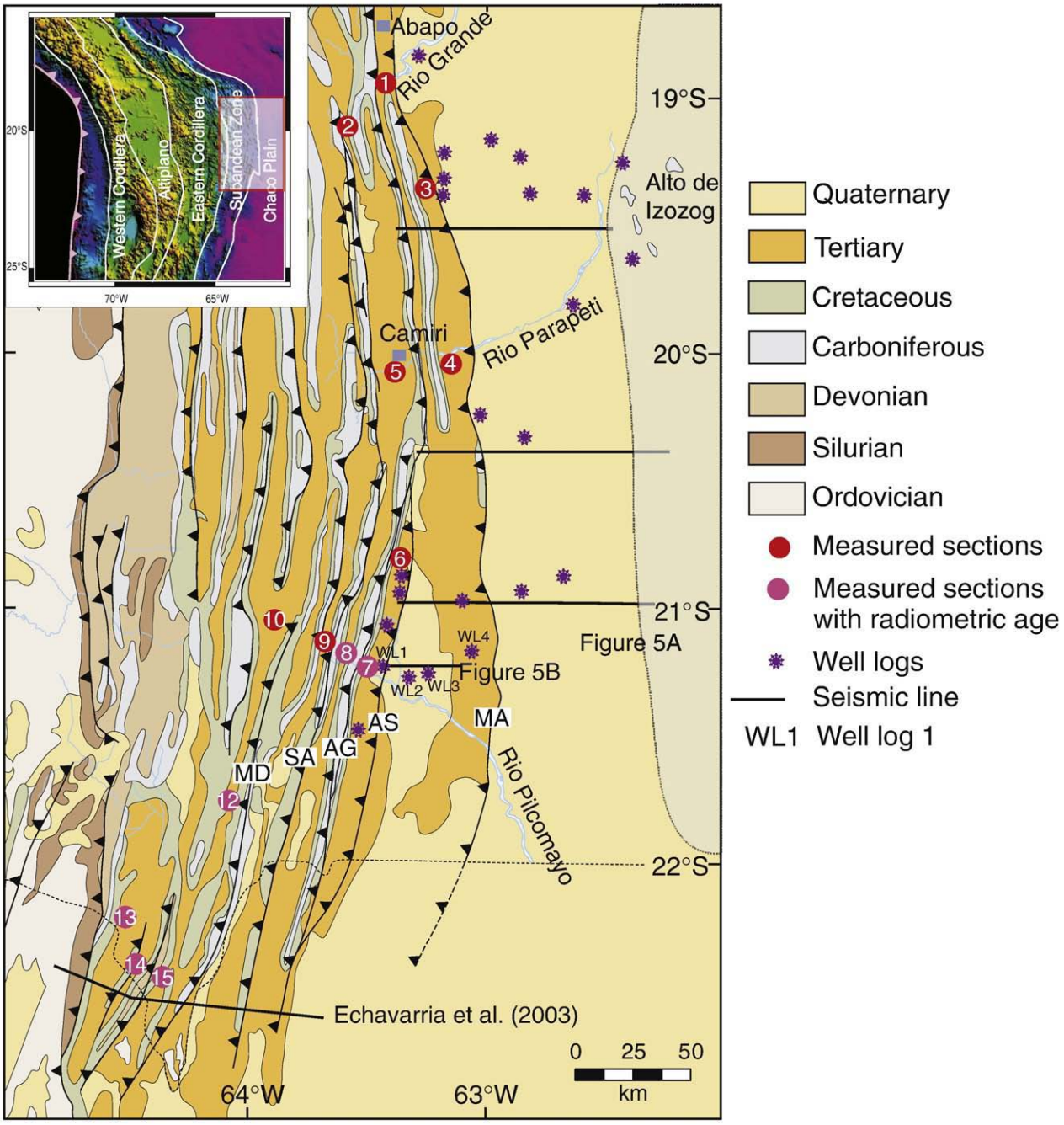

Fig. 1. Digital elevation map of the central Andes with the principal morpho-structural provinces and the location of the study area (inset) and the geological and structural map of the study area showing the location of measured sections, measured sections with radiometric ages, well-log data, and seismic profiles used in this study: 1, Abapo; 2, Tatarende; 3, Saipuru; 4, San Antonio; 5, Itapu; 6, Machareti; 7, Angosto del Pilcomayo; 8, Puesto Salvación; 9, Zapaterimbia; 10, Rancho Nuevo; 11, Sanadita; 12, Chiquiaca; 13, Emborozú; 14, Nogalitos; 15, San Telmo; MA, Mandeyepecua Fault; AS, Agua Salada; AG, Aguarague range; SA, San Antonio; MD, Mandiyuti Fault.

of the Brazilian Shield under the orogen (e.g., Isacks, 1988; Sempere et al., 1990; Kley et al., 1997) led to widespread and pronounced thrusting in the Eastern Cordillera in the Oligocene; subsequently, deformation migrated eastward into the Subandean region during the late Miocene (Baby et al., 1992; Gubbels et al., 1993; Horton, 1998; Uba et al., 2006; Ege et al., 2007). According to DeCelles and Horton (2003), the Andean foreland fold-and-thrust belt migrated to its present location at rates of 12–20 mm/yr. Most shortening in the central Andes has been concentrated in the Subandes during the last 10 Ma (Gubbels et al., 1993; Moretti et al., 1996; Kley et al., 1999; Echavarria et al., 2003). The growth of the thrust wedge has caused the eastward younging of depozones (DeCelles and Horton, 2003; Uba et al., 2006) and sediment pinch-out migration (Uba et al., 2006).

There are marked changes in morphology from the rugged Interandean zone with its steep-walled, deeply incised valleys to the N–S trending valley-and-ridge topography of the Subandean belt, and finally the low-elevation Chaco plain of the foreland to the east (Fig. 1). The Subandean belt is characterized by thin-skinned, partially blind thrusting and folding (Baby et al., 1992; Dunn et al., 1995; Kley et al., 1996; Horton and DeCelles, 1997; Uba et al., 2006). Coudert et al. (1995) and Echavarria et al. (2003) postulated a three-phase subsidence and deformation history in the Subandean belt beginning at 10 Ma. The estimated total shortening in the Subandes ranges between ca. 60 and 86 km (Baby et al., 1997; Kley et al., 1997; Echavarria et al., 2003).

The late Cenozoic lithostratigraphy of units exposed in the Subandes and the foreland is illustrated in Fig. 2. Sedimentation in these areas started during the late Oligocene, when the Eastern Cordillera was undergoing deformation (Sempere et al., 1990; Uba et al., 2006). This deformation and its subsequent eastward migration led to the accumulation of up to 7.5 km of mostly siliciclastic sediments (Uba et al., 2006). The base of the late Cenozoic strata is characterized by the 200-m-thick, 26 to 12.4-m.y.-old Petaca Formation. This unit consists of conglomerate, sandstone, and mudstone that accumulated in a fluvial environment; in addition, this thin unit contains a thick paleosol record (Uba et al., 2005). Overlying the Petaca Formation is the 500-m-thick Yecua Formation. This unit consists of mudstone and calcareous sandstone deposited in a transitional environment between lacustrine, fluvial, and marine settings (Uba et al., 2005, 2006). U–Pb dating of a tuff at the base of the Yecua Formation provided an age of 12.4 Ma ± 0.5 (Uba et al., 2007).

The Yecua Formation is overlain by the up to 3000-m-thick Tariquia Formation, which is 8 to 6 m.y. old. This sandstone- and mudstone-dominated formation represents deposition in a distal fluvial megafan. These deposits grade into the up to 1500-m-thick Guandacay Formation. The 5.94–2.1 m.y-old Guandacay Formation consists of sandstone, conglomerate, and subordinate mudstone deposited in a medial fluvial megafan environment (Uba et al., 2005, 2006). This late Cenozoic succession is capped by the more than 1500-m-thick, 2.1 Ma to Present Emborozú Formation, which is composed of conglomerate, sandstone, and sandy mudstone deposited in a proximal fluvial megafan environment (Uba et al., 2005).

3. Methods and results

3.1. U–Pb geochronology and Neogene chronostratigraphy

We dated eight volcanic ashes interbedded in the Mio-Pliocene strata (Yecua, Tariquia, Guandacay, and Emborozú formations) in the central Subandean zone. The volcanic ash samples were obtained from the Emborozú, Nogalitos, San Telmo, and Chiquiaca sections (Fig. 1 shows location). These sections are located west of the dated stratigraphic profiles of Uba et al. (2007). The zircon samples were dated with U–Pb geochronology by secondary ionization mass spectrometry (SIMS, ion microprobe) using the Cameca ims 1270 at UCLA. For each of the samples, the ashes were crushed, sieved and the zircons were separated using standard heavy-liquid procedures and magnetic separation techniques.

About 10–20 zircons per sample were handpicked and placed on epoxy mounts, which were then polished and gold-coated for analysis. A ~15 nA O^- primary beam with 22.5 keV total impact energy was focused to a ~25 μm diameter spot. Secondary ions were extracted at 10 kV with an energy band pass of 50 eV. O_2 pressure in the sample chamber was adjusted to ~0.002 Pa, which increased Pb sensitivity by ~50%. In four analytical sessions between August 2006 and November 2007 the reproducibility of $^{206}Pb/^{238}U$ ages of reference

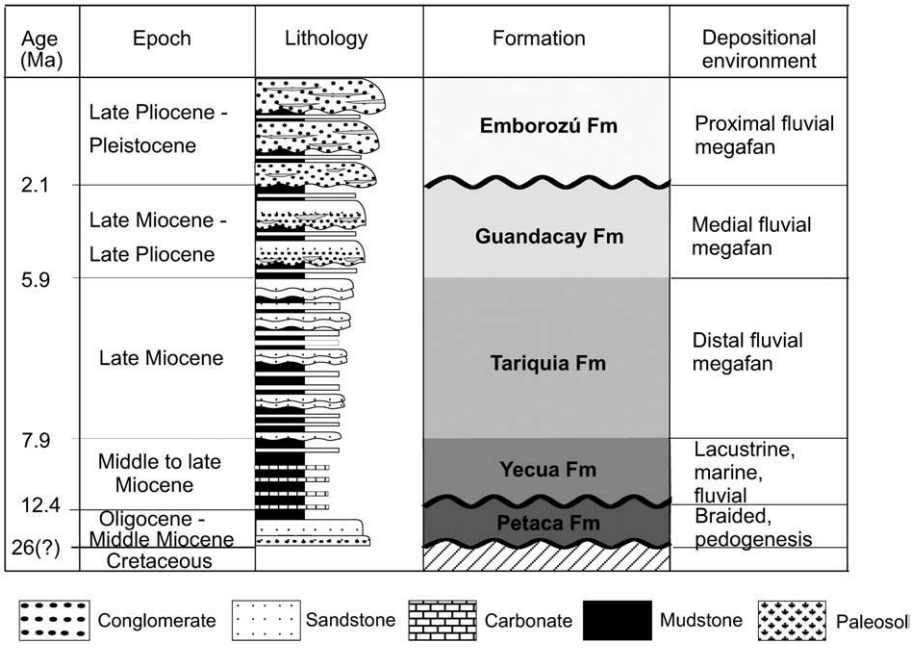

Fig. 2. Late Cenozoic lithostratigraphy of the Subandean fold and thrust belt at the Angosto de Pilcomay-Puesto de Salvación region. The ages of the base Petaca and Emborozú formations are based on Marshall and Sempere (1991) and Hulka (2005) respectively. The remaining ages are after Uba et al. (2007). The lithology shows an overall thickening and coarsening-upward sequences. The depositional environments are based on Uba et al. (2005, 2006).

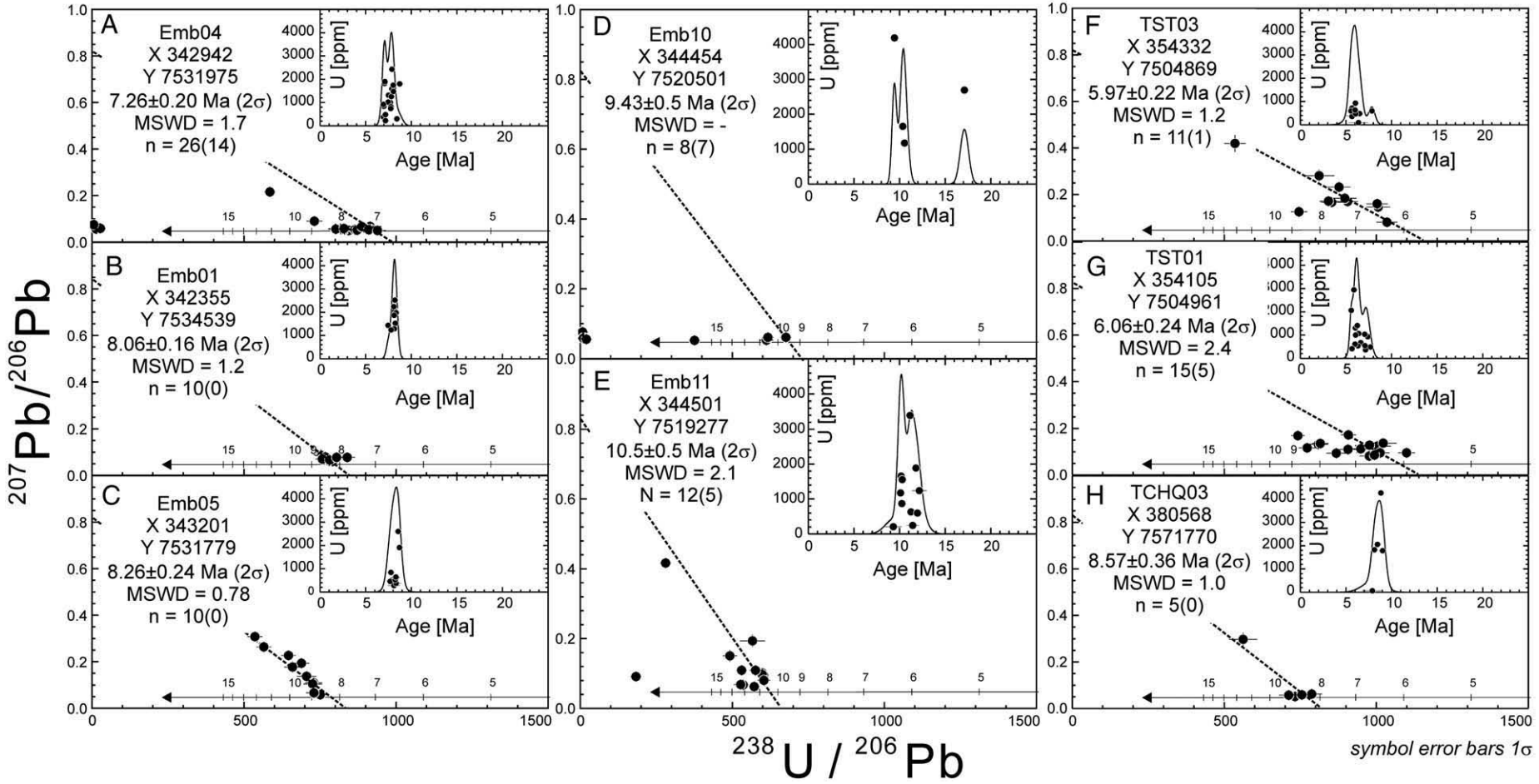

Fig. 3. A summarized Tera-Wasserburg plots showing our new 8 U–Pb radiometric ages recorded in the Yecua, Tariquia, Guandacay, and Emborozú formations at the Emborozú (Emb 01, 04, 05), Nogalitos (Emb 08, 11), San Telmo (ST 01, 03), and Chiquiaca (Chq 01) sections.

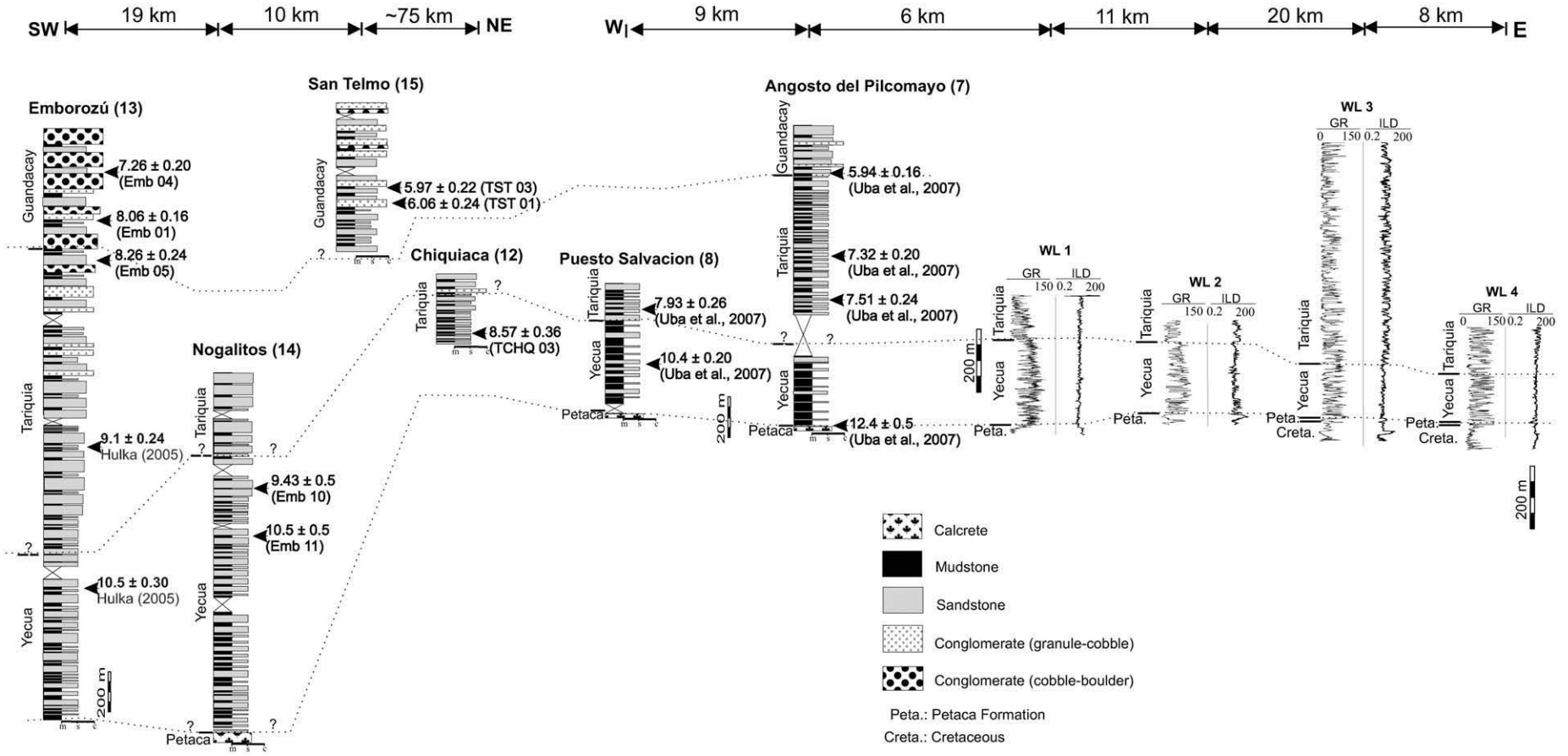

Fig. 4. Correlated SW–NE-oriented measured stratigraphic profiles showing in each column the location of the U–Pb ages used in this study and correlated well logs. The figure shows westerly diachronous pattern for the Neogene sedimentation. Furthermore, it shows thickening- and coarsening upward trend, westward increase in sandstone and conglomerate proportion, upsection and westward decrease in mudstone proportion.

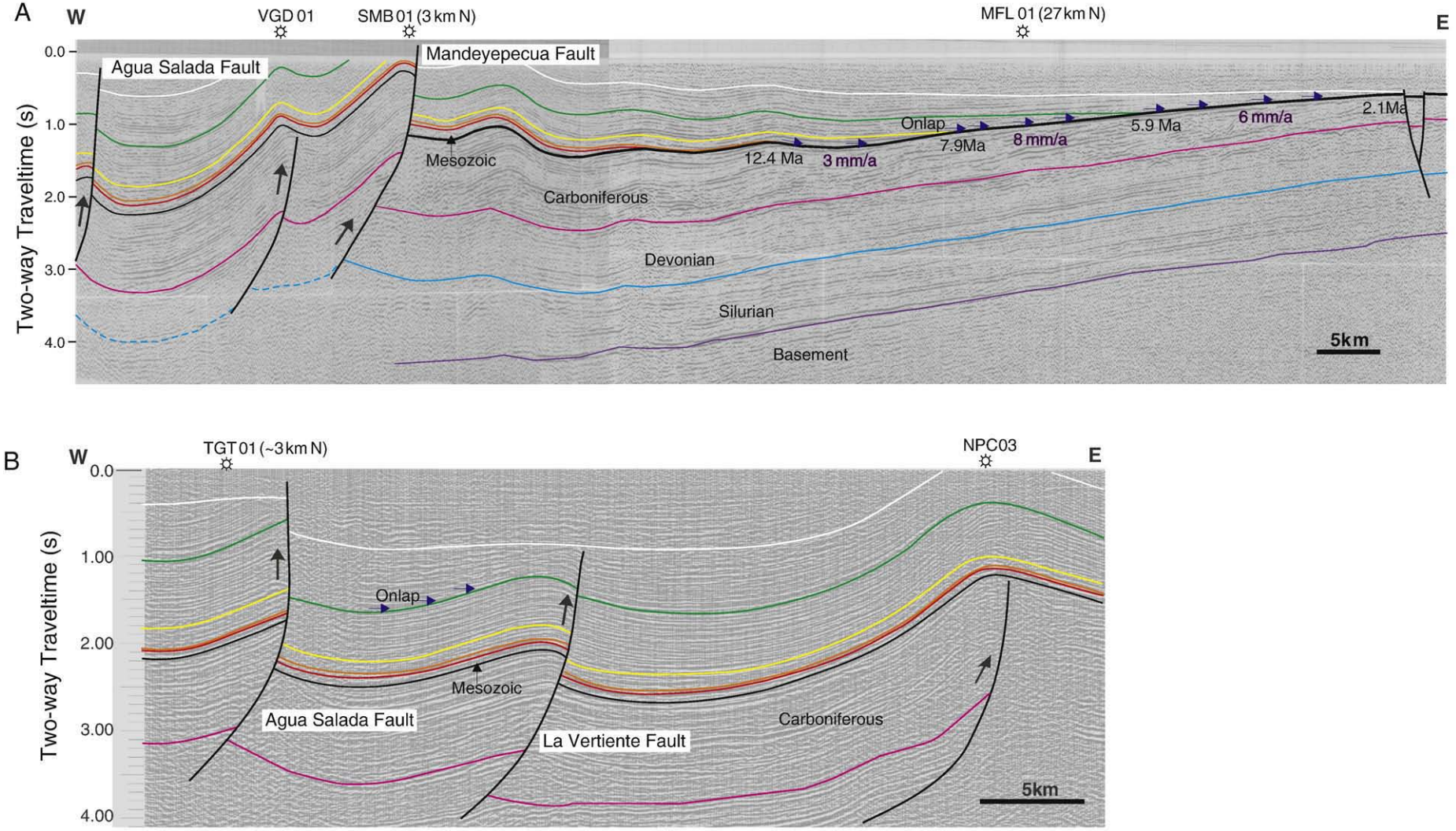

Fig. 5. (A) Interpreted W–E reflection seismic profile (see Fig. 1 for location) showing deposition pinch-out, onlap, and downlap reflection terminations of base Petaca (red line), base Yecua (orange line), base Tariquia (yellow line), base Guandacay (green line), and base Emborozú (white line) formations on the Alto de Izozog. In contrast, the pre-Mesozoic successions do not show reflection terminations on this structure. The figure shows the estimated amount and rates of deposition pinch-out migration for the three intervals namely, 12.4–8 Ma (Yecua Fm.), 8–6 Ma (Tariquia Fm), and 6–2.1 Ma (Guandacay Fm). The ages used to constrain the bases of the formations are from the nearest U–Pb ages at the Angosto de Pilcomayo section. (B) Interpreted W–E reflection seismic profile showing the structural styles and growth structure as a result of La Vertiente Fault documented by onlap terminations of Guandacay strata.

zircon AS-3-, was ~2.8% (1 standard deviation). All U–Pb ages were corrected for initial ^{230}Th deficit using measured zircon U/Th and whole-rock U/Th = 2.3 (central Andean ignimbrite average; Schmitt et al., 2002). This correction typically adds ~0.1 Ma to the equilibrium ^{206}Pb/^{238}U ages. Due to extremely slow diffusion of U and Pb in zircon, crystallization ages are essentially unaffected by pre-eruptive crystal storage even at elevated temperatures. Detrital contamination typically results in complex zircon age distributions (e.g., Schmitt et al., 2002), whereas zircon-age spectra with a single dominant age peak indicate minor assimilation or reworking.

The Ion microprobe results for the samples are summarized in Tera-Wasserburg plots in Fig. 3 and in the Data Repository[1] in Appendix A. These ages, which range between 5.97 ± 0.22 Ma and 10.5 ± 0.5 Ma, complement the ages documented by Uba et al. (2007) for this region and those presented by Echavarria et al. (2003) in northeastern Argentina. Importantly, this data helps constrain for the first time the depositional ages for the late Cenozoic strata in the western part of the Subandean zone in Bolivia, particularly the base of the Guandacay (8.26 ± 0.24 Ma) and Tariquia (10.5 ± 0.5 Ma) formations, respectively (Fig. 3). Because the chronostratigraphy of the late Cenozoic strata was previously poorly constrained, these new ages help better define both the chronostratigraphy of the deposits in the Bolivian Subandes and the timing of deformation.

Fig. 4 shows the correlation of the new ages and previously published radiometric ages in the study area (Uba et al., 2007). The 8.57 ± 0.36 Ma volcanic ash was deposited prior to the onset of the deposition of conglomerates with Andean provenance (Hulka, 2005; Uba et al., 2005, 2006). Combined with the sedimentologic and basin analysis (Uba et al., 2005, 2006), this suggests that during this time the western Subandean basin was adjacent to elevated areas farther west, from where clasts were transported into the system. Possibly, the deposition of these strata may have taken place in a piggy-back basin in the eastern Interandes(?) or western Subandes, as the region was subjected to eastward propagation of deformation at that time. In contrast, the 10.5 ± 0.5 Ma ash interbedded in coarse-grained sandstone lies more than 1100 m above the base of a lateral equivalent of the Yecua Formation, suggesting a 10.5 ± 0.5 Ma minimum age for the base of this unit at this location.

3.2. Depositional pinch-out migration

We reconstruct the long-term migration rate of depositional pinch-outs onto the western flank of the NNE–SSW-oriented Alto de Izozog basement high in the eastern foreland using industry-seismic-reflection profiles provided by Chaco S.A., Bolivia. With up to 800 m elevation, the Alto de Izozog is a pre-Mesozoic paleo-high (Uba et al., 2006) associated with toplap, downlap, and onlap reflector terminations (e.g., Mitchum et al., 1977; Hubbard et al., 1985) of late Cenozoic sedimentary units. Lithologic control for the seismic stratigraphic units was attained through well-log correlation (Uba et al., 2006) and augmented by 15 outcrop sections.

We used four W–E-oriented seismic reflection profiles, tied to well logs (Fig. 1) and outcrops, to distinguish five late Cenozoic sequences through delineation of discontinuities on the Alto de Izozog. Lateral correlations and seismic attributes used include prominent reflectors, reflection configuration, onlaps, toplaps and truncation, documented by Uba et al. (2006). In addition, the five sequences are delineated by discontinuities that coincide with changes in seismic facies, also documented by well-logs (Fig. 5). The ages of the Cenozoic sequences imaged on the seismic profiles are inferred through correlation with the nearest dated Tertiary units exposed in the well-constrained Angosto del Pilcomayo section (Fig. 4). Thereafter, we measured the distances between the Yecua, Tariquia, and Guandacay formations, which define the amount of deposition pinch-out migration. We focused on these three well-constrained units because of the poor age constraints for the Petaca and Emborozú units.

We acknowledge the possibility that the Alto de Izozog might have experienced minimal uplift during the late Cenozoic, nonetheless, we assume that vertical movements were below the degree of uncertainty, thus not large enough for having significantly influenced our results. This assessment is based on the documented eastern pinch-out termination of all Neogene strata with the exception of the upper part of the younger Emborozú Formation (Fig. 5A and Data Repository[2] in Appendix A). Consequently, the Izozog High has been a stationary ridge since pre-Mesozoic time that cannot be explained in terms of uplift in the forebulge area. This led Uba et al. (2006) to suggest that it cannot have originated as a Neogene flexural forebulge, although it was probably somewhat accentuated by flexural uplift. This is indicated by the slight westward dip of the Neogene units. Our pinch-out migration estimates thus reflect foreland basin subsidence, but not the free migration rate of an ideal, flexural wave (DeCelles and DeCelles, 2001).

The deposition pinch-out migration rates for the Yecua (12.4 to 8 Ma), Tariquia (8 to 6 Ma), and Guandacay (6 to 2.1 Ma) formations do not vary much between the three N–S seismic profiles (Fig. 5A and Data Repository[2] in Appendix A). However, in each profile the rates vary upsection. Each section begins with an initial low pinch-out migration rate of 3 mm/a between 12.4 and 7.9 Ma, followed by an almost three-fold increase to 8 mm/a during the 7.9 to 5.9 Ma interval, and finally a decrease to 6 mm/a between 5.9 and 2.1 Ma (Table 1A).

Earlier pinch-out migration rates for more internal areas of the Subandean foreland basin can be estimated from our new age data in the western Subandes. The base of the Tariquia formation migrates from the Emborozú section to the Puesto Salvación section between ca. 10 and 8 Ma (Fig. 4), and the base of the Guandacay Formation migrates from the Emborozú section to the Angosto del Pilcomayo section between 8.5 and 5.9 Ma. With original distances measured from restored cross-sections (see below) and not taking into account possible along-strike age variations, this corresponds to migration rates of ca. 37 mm/a for the Tariquia and ca. 28 mm/a for the Guandacy formations. These rates are substantially faster than those measured farther east from the seismic lines, but agree with regards to indicating an exceptionally high pinch-out migration rate for the strata associated with the Tariquia Formation.

3.3. Rates of thrust-front propagation and shortening

Propagation of a thrust front toward the foreland can be estimated from stepwise-restored cross-sections if the nucleation ages of

Table 1A

	Age (Ma)	Formation	Pinch-out distance (km)	Estimated age of the basal (Ma)	Migration rate (mm/a)
Line 5013	5.9–2.1	Guandacay	30.4	3.8	7
	7.9–5.9	Tariquia	20.1	2	9
	12.4–7.9	Yecua	15	4.5	3
Line 4568	5.9–2.1	Guandacay	25.5	3.8	7
	7.9–5.9	Tariquia	16.8	2	8
	12.4–7.9	Yecua	12	4.5	3
Line 4506	5.9–2.1	Guandacay	22.1	3.8	6
	7.9–5.9	Tariquia	15.1	2	8
	12.4–7.9	Yecua	14.4	4.5	3

individual thrusts are known. Balanced cross-sections of the Subandean transect discussed here (c. 21° 20' S latitude) were published by Dunn et al. (1995) and Moretti et al. (1996). Both interpretations are based on essentially the same geological map and some industry seismic data, although the work by Dunn et al. (1995) includes a more complete documentation of the database. Both studies show very similar near-surface structure, but different architecture at depth. Bulk Subandean shortening of the two interpretations is 61 km and 78 km, respectively, providing some indication of the error of these shortening estimates. An important structural feature of the section of Dunn et al. (1995) is a second detachment in Devonian shales above the basal detachment in Silurian strata. The second detachment links adjacent structures, and the restoration requires at least two major thrust faults to have been active simultaneously at any time. However, Echavarria et al.'s (2003) interpretation of corresponding structures some 140 km farther south demonstrates that this is not a necessary assumption. Also, at 60 km their shortening value is practically identical. We therefore simplified the deep structure of Dunn et al.'s (1995) cross-section to be more in line with Echavarria et al.'s (2003) section near 22°30'S. We then used this section to measure line lengths with the relatively shallow Carboniferous interval as a marker and constructed a step-by-step evolution. However, as the details of the deep structure are of no importance for the problems discussed here and no new data were available, we made no effort to perfectly balance line lengths and areas at depth.

We used the new age results from this study in combination with published U–Pb and Ar–Ar ages for the Yecua, Tariquia, and Guandacay formations (Uba et al., 2007) and the Emborozú Formation (Hulka, 2005) to constrain the timing of deformation and thus, estimate the rates of propagation and shortening. We used the onset of the deposition of cobble–boulder conglomerates and growth structures (Uba et al., 2006) at the Emborozú and San Telmo sections to indicate the transition from a foredeep to a wedge-top environment and the onset of local deformation. Due to the still localized age control, we can only pinpoint the initiation ages of the Western Subandes and the Mandiyuti, La Vertiente and Aguaragüe structures.

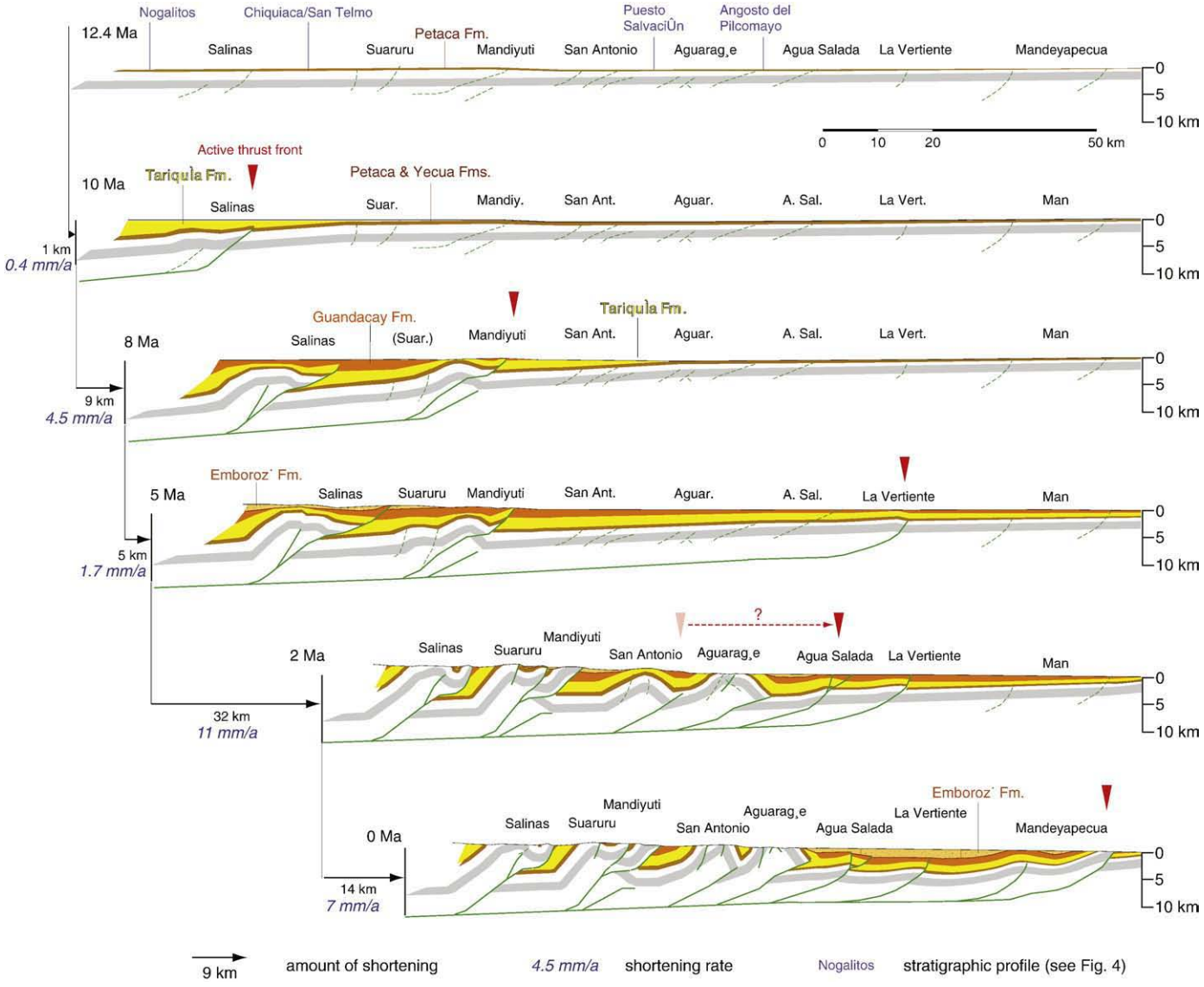

Fig. 6. Structural evolution scheme of the Subandean thrust belt and associated foreland deposits in southern Bolivia. Near-surface structure is after Dunn et al. (1995). The onset of deformation on individual structures is taken from sedimentological and new geochronologic evidence as discussed in the text. Further evolution of the anticlines is partially constrained by conformable strata on their backlimbs. Notice forelandward shift of deformation front to the La Vertiente structure around 5.5 Ma, followed by retreat and renewed propagation from around 2 Ma. The Carboniferous to Triassic interval is shown as a structural marker (grey). Deep structure is simplified from Dunn et al. (1995) and not strictly balanced.

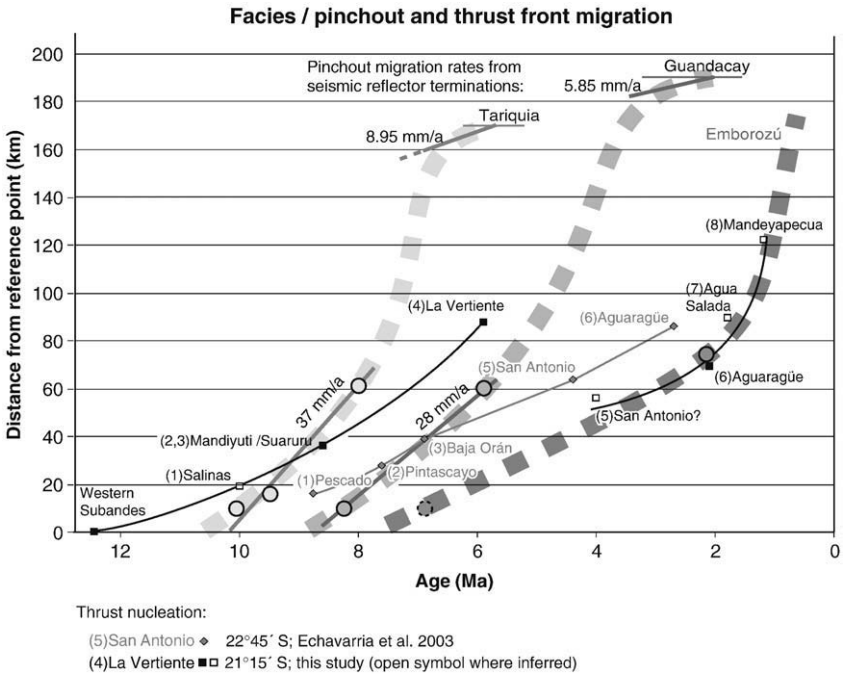

Fig. 7. Comparison of thrust front propagation (thin lines) and facies/deposition pinch–out migration rates in our transect and another one further south (Echavarria et al., 2003). Numbers next to structure names indicate structural correlation between the two transects. Our data suggests two pulses of thrust front propagation at rates similar to coeval facies/pinch out migration. Linear pinch–out migration rates calculated from seismic reflector terminations in the foreland (top) and from dated formation boundaries in the Subandean sections (circles) are shown. Thick, dashed curves show pinch–out migration histories for the Tariquia (left), Guandacay (center), and Emborozú (right) formations as inferred from interpolation of the Subandean and foreland rates.

We commenced our structural model at 12.4 Ma based on the well constrained age of the base of the Yecua Formation in the Pilcomayo section (Fig. 6). Older units are poorly constrained. The onset of the La Vertiente structure is well constrained by the 5.9 (~6) Ma volcanic ash at the base of the Guandacay Formation coinciding with the initiation of growth strata (Fig. 5B). Age estimates for the remaining structures were made by interpolation. On a time vs. propagation distance plot, propagation rate curves were determined from the well-dated structures (Fig. 7). Ages for specific propagation distance values corresponding to particular structures were then read off these curves. This exercise suggests a scenario with two accelerating propagation pulses: the first migrated from the Western Subandes to the well-dated La Vertiente structure between 12.4 and c. 6 Ma, and a second one started west of the older thrust front and migrated from the San Antonio structure to the present deformation front at Mandeyapecua between ca. 4 and <2 Ma (Fig. 6 and Table 1B).

Determining variations in the shortening rate of the Subandean belt remains difficult despite improved chronologic and stratigraphic control of the foreland-basin succession. The major problem is that the termination of activity on each structure is in most cases only poorly constrained by the youngest strata involved. This allows for a wide range of rate estimates, particularly for the formation of the older structures. Echavarria et al. (2003) therefore calculated two end-member models: one for a minimum and one for a maximum duration of activity for each thrust, resulting in two shortening peaks or steadily accelerating shortening, respectively. They preferred the two-peak model because it agrees with the two-peak subsidence model of Coudert et al. (1995). Our dataset, which has better radiometric age control, but is less continuous than the magnetostratigraphic record of Echavarria et al. (2003), however, does not provide better upper age limits for the activity of individual structures.

We have therefore combined all available data on the diachronous formation and facies migration, shortening magnitudes, growth strata and the present-day GPS-based shortening rate to constrain a stepwise forward model of our cross-section (Fig. 6). The number of time steps warranted by the data is limited, and there is some uncertainty as to their exact ages. For some structures, part of the shortening could also be shifted to another time step. This is why the absolute values of the shortening rates given in Figs. 6 and 8 should be viewed with care. However, one important constraint comes from the conformable successions on the backlimbs of most structures. Unless we assume that all Subandean deformation is younger than the Tariquía or even Guandacay formations (i.e. <~6 Ma), the implication is that originally present growth sections were uplifted and eroded during later, continuous or intermittent deformation (Fig. 6). Scenarios where all structures remain active throughout the evolution of the Subandean belt tend to predict (sub-)recent shortening rates much higher than measured today. Thus, a two-pulse pattern with an intervening phase of low shortening rates similar to those proposed by Moretti et al. (1996) and Echavarria et al. (2003) is favorable. In any case, there is no indication of particularly high shortening rates in the 8–6 Ma interval.

In summary, our reconstruction suggests that the upsection variation in shortening rates does not mimic the variation in thrust front propagation- and deposition migration rates in the Subandes. This observation points to additional, non-tectonic processes

Table 1B

Structure	Age (Ma)	Distance from reference point (km)	Distance propagated in this time step (km)	Time lapse (Ma)	Propagation rate (km/Ma)
Sama	30	0			
Interandean	16.5	63	63	14.5	4.3
Western SA	12.4	126	63	4.1	15.4
Pescado	10	187	61	2.4	25.4
Suaruru/ Mandiyuti	8.6	224	37	1.4	26.4
La Vertiente	6.1	307	83	2.5	33.2
San Antonio	4	258	−49	2.1	−23.3
Aguaragüe	2.1	289	31	1.9	16.3
Mandeyapecua	1.5	342	53	0.6	88.3

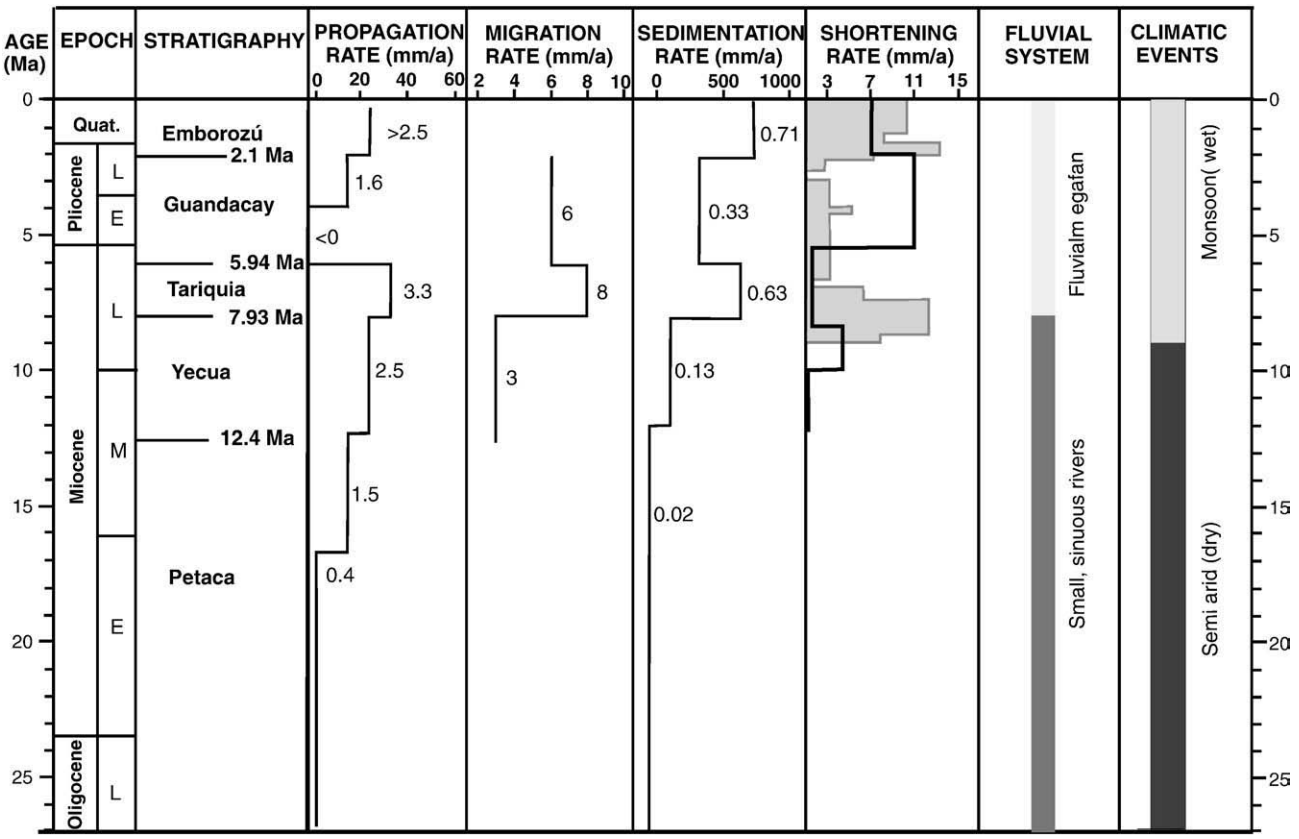

Fig. 8. Summary chart of propagation rate, average deposition pinch-out migration rate from the southern-most seismic profile (Fig. 5A) that is adjacent to the ages used, sedimentation rate at the Angosto del Pilcomayo section (Uba et al., 2007), shortening rate (this study: red curve; Echavarria et al., 2003: pink diagram), fluvial system characteristic (Uba et al., 2005), and climatic event (Strecker et al., 2006). The numbers beside the curves show the actual values. The figure shows a three- and four-fold increase in deposition pinch-out and sediment accumulation rates respectively, coupled with two-fold increase in propagation rate at 8–6 Ma. Increase in rate during this time coincides with the decrease in shortening rate and change in drainage system and South American monsoon intensification. (For interpretation of the references to colour in this figure legend, the reader is referred to the web version of this article.)

controlling the evolution of the Subandean thrust belt. The strongest difference is observed at 8–6 Ma, when the rates of pinch-out migration and thrust front propagation are almost four- and two-fold the shortening rate.

4. Discussion and conclusions

4.1. Comparison of thrust-front propagation with the Subandes of Argentina

We compare our thrust-front propagation estimate to published data from northwestern Argentina (Echavarria et al., 2003) in the south, which reveals some differences (Fig. 7). The southern transect (Echavarria et al., 2003) has a very regular sequence of fault nucleation with the thrust wedge growing to a length of 86 km from ca. 9 to 2.7 Ma. In our transect, the details of eastward propagation are not as well documented. However, growth strata associated with the La Vertiente structure demonstrate that the wedge had already attained a length of 88 km by ~6 Ma. This propagation pulse and the following westward shift of the active thrust front are not recorded in the southern transect. This may be due to the fact that the La Vertiente structure does not extend much farther to the south and structures east of the Aguaragüe anticline were not included in the analysis of Echavarria et al. (2003). During the first phase of thrust propagation, there is a systematic time lag of ca. 1.5 Ma in the onset of thrusting on the southern transect. In general, some time lag would be expected from the location of the northern transect closer to the center of the arcuate Subandean belt. Nevertheless, no time lag seems to exist for the nucleation of the younger, more easterly structures.

With regards to shortening rates, Echavarria et al. (2003) proposed two rapid shortening pulses around 9–7 Ma and during the ultimate 2 Ma, separated by a period of low shortening rates between 7 and 2 Ma. Our results also suggest two shortening pulses, but with a shift of the two-peak pattern to a higher age by 2–4 Ma, and a longer duration of the younger pulse. These substantial differences emphasize that data from one transect cannot be simply extrapolated to other sectors within the same morphotectonic province of the Andean orogen. An important observation is that neither estimate has a shortening pulse coinciding with the rapid advance of deposition between 8 and 6 Ma.

4.2. Timing of earliest deformation in the Subandean ranges

Gubbels et al. (1993) used the ~10 Ma age of the San Juan del Oro erosional surface in the Eastern Cordillera to date the end of thrusting in the Eastern Cordillera and the subsequent onset of activity along the deformation front in the Subandean zone. In contrast, Echavarria et al. (2003) interpreted the rapid increase in sedimentation rate around ~9.9 Ma to indicate the onset of deformation in the Subandes. The age used by Echavarria et al. (2003) was from a volcanic ash ~1200 m above the top of the Tranquitas Formation. Marshall and Sempere (1991) and Uba et al. (2006) related the onset of deformation in the Subandean zone to the commencement of the deposition of the Yecua Formation based on biostratigraphic and sedimentologic studies. However, McQuarrie et al. (2005) invoke the cessation of significant shortening and thickening related to motion on an extensive basement megathrust within the Interandean zone at ca. 20 Ma to suggest a pre-13 Ma onset of deformation within the Subandean belt. This interpretation of an earlier onset of tectonism is further supported by apatite

fission track ages (Ege, 2004; Ege et al., 2007) and structural studies aided by radiometric dating (Horton, 2005).

Notwithstanding the above controversy on timing, it is generally agreed that the initiation of deformation within the Subandean zone was coeval with the onset of deposition of the Yecua Formation (e.g., Marshall and Sempere, 1991; Baby et al., 1992; Marshall et al., 1993; Gubbels et al., 1993; Dunn et al., 1995; Kley et al., 1997; Uba et al., 2005, 2006). The correlation of the onset of deformation in the Subandes with commencement of Yecua sedimentation is based on an increase in shortening rate (Gubbels et al., 1993; Moretti et al., 1996; Echavarria et al., 2003), high subsidence rate, and creation of accommodation space (Coudert et al., 1995; Uba et al., 2006). In addition, the deposition of marine–lacustrine facies (Uba et al., 2005, 2006), rapid cooling based on apatite fission-track analysis (Ege, 2004), and a low-angle unconformity over the underlying Petaca Formation (Uba et al., 2006) have been used to infer the onset of deformation and the contemporaneous deposition of the Yecua Formation. In light of our new radiometric age of 12.4 Ma at the base of the Yecua Formation in the Angosto del Pilcomayo section and 10.5 Ma in the upper part of the same unit in the Emborozú section, we are able to better constrain the onset of deformation in the western Subandean zone to 12.4 Ma. This correlates with rapid increases in the shortening and subsidence rates as demonstrated in our study, which is compatible with the creation of accommodation space for the coeval deposition of lacustrine and shallow marine units.

Subsequently, thrusting was mostly transferred to the central Subandean zone in the Mandiyuti range at 8.6 Ma (Fig. 6), as reflected by the Chiquiaca and Emborozú sections. Our data shows that this period with a low shortening rate was followed by a rapid increase in wedge propagation to the La Vertiente structure at 6 Ma (Fig. 6). This marks the onset of the second major phase of thrusting. However, most of the deformation was apparently accommodated by out-of-sequence thrusting on the San Antonio and Aguaragüe structures (Fig. 6). This agrees with similar observations in northeastern Argentina (Echavarria et al., 2003).

4.3. Erosion and evolution of topography in the Subandes

A faster sediment accumulation of 0.63 mm/a at 8–6 Ma after a protracted episode with low rates on the order of 0.13 mm/a between approximately 12.4 and 8.6 Ma has been documented in the Subandes and was attributed to an intensification of the South American monsoon system and associated climate variability (Uba et al., 2007). In that scenario a shift toward higher precipitation would have caused higher stream competency and increased erosion, sediment transport, and sediment supply to the basin. Sediment accumulation rates are primarily a proxy for subsidence and the creation of accommodation space. However, the increased sediment accumulation rate between 8 and 6 Ma coincided with changes in fluvial depositional styles from small rivers to fluvial megafans with frequent avulsion, channel abandonment, and progradational sequences (Uba et al., 2005), suggesting that sediment supply kept up with the increased subsidence rate. Based on these premises, the central Andes in our transect probably witnessed an up to four-fold increase in erosion between 8 and 6 Ma. In addition, a climate-driven increase in erosive processes is in line with thermochronologic studies (e.g., Ege, 2004; Barnes et al., 2006), suggesting rapid exhumation in the Interandean and the Subandean belt since the late Miocene. At 6 Ma, the accommodation space was largely filled due to high sediment accumulation during the preceding period, resulting in increased bypassing of sediment during the deposition of the Guandacay Formation between 6 and 2.1 Ma (Uba et al., 2005).

Paleoclimatic studies suggest that precipitation in the Eastern Cordillera decreased in the last 10 Ma (e.g., Graham et al., 2001). Reduced precipitation in the Eastern Cordillera and coeval rapid erosion in the Interandean and probably western Subandean zone since 8 Ma are compatible with the creation of an orographic barrier in the Eastern Cordillera after it had attained sufficient elevation to cause a rain shadow, similar to observations in the Eastern Cordillera of northwestern Argentina (Starck and Anzótegui, 2001; Kleinert and Strecker, 2001; Strecker et al., 2007). This situation suggests that rainfall related to the South American monsoon exerted a strong control on surface erosion processes that began to effectively incise and erode the thrust belt, evacuating sediments into the foreland basin.

Low shortening and subsidence rates at 8 to 6 Ma in the study area (this study; Coudert et al., 1995; Echavarria et al., 2003) are evidence for only minor deformation, thus suggesting that thrusting activity in the Interandean and western Subandean zone between 12.4 and 8 Ma should have led to the development of an efficient orographic barrier by ~8 Ma and the formation of the San Juan del Oro erosion surface (e.g., Baby et al., 1992; Gubbels et al., 1993; Kley et al., 1997).

4.4. Implications for central Andean geodynamics

The Neogene sedimentary units in the Subandes of Bolivia reflect wedge propagation, shortening, deposition pinch-out migration, and a migration of erosion patterns in the Subandean fold and thrust belt. Our study sheds some light on the possible mechanism(s) controlling the evolution of the central Andes. Fig. 8 shows a compilation of propagation, deposition pinch-out migration, and shortening estimates, documenting that between 12.4 and 8 Ma the fold and thrust belt witnessed an increase in propagation- and shortening rates, but with low rates of pinch-out migration and sediment accumulation. These are indications of enhanced deformation and development of topography in the Interandean and western Subandean zones. Topographic growth is further supported by geomorphic data along the same transect to the west, documenting surface uplift of ca. 1700 m during this time (Barke and Lamb, 2006).

Surface uplift suggests crustal thickening in the Interandean and probably western Subandean zones. Crustal thickening induced subsidence in the eastern Subandes (Coudert et al., 1995; Echavarria et al., 2003) that probably outpaced the ability of the regional depositional systems to fill the accommodation space created during this time. Thrusting was accompanied by low deposition pinch-out migration- and accumulation rates. This implies high flexural loading of the Brazilian Shield and the Subandean basin, and suggests an important phase of forelandward growth of the Subandean ranges in the interval between 12.4 and 8 Ma.

In contrast, between 8 and 6 Ma, our data indicates an increase in the rates of deposition pinch-out migration, propagation, and sediment accumulation. This was accompanied by a low shortening rate or at least not by a discrete shortening pulse (Fig. 8). This time interval is also marked by a rapid increase in erosion and transport efficiency. We interpret this increase in sediment flux to be the result of enhanced precipitation of the South American monsoon driving erosional unloading of the internal parts of the fold-and-thrust belt, which exceeded the volume of rock advected by crustal thickening. We hypothesize that the unloading observed in the Subandes between 8 and 6 Ma probably caused flexural rebound of the thrust belt and lateral expansion of the foreland basin, similar to modelling results by Flemings and Jordan (1990).

DeCelles and Mitra (1995), Willett (1999), Watts (2001), and Whipple and Meade (2006) have shown that removal of mass due to enhanced erosion would be regionally compensated by flexural uplift of the underlying plate, leading to flexural rebound. In addition, strikingly similar erosion-induced mass reduction and flexural rebound have been reported from the Alps (Schlunegger and Simpson, 2002; Cederbom et al., 2004) and the Himalaya (Huyghe et al., 2001). For example, Huyghe et al. (2001) have shown that outward migration of deposition pinch-out in the Himalayan foreland could record the foreland-ward motion of the thrust wedge or flexural rebound of the

thrust belt as a result of erosion-induced reduction in topography. The coincidence of the three-fold increase in deposition pinch-out migration rate in the Subandes between 8 and 6 Ma coupled with a four-fold increase in sediment accumulation rate suggests close relationship between subsidence and eastward migration of deposition pinch-outs in the foreland.

In our transect, the progradation of the fluvial megafan is followed by rapid propagation of the thrust front to the well-dated La Vertiente structure. However, the shortening accommodated on this thrust front is very low, and the focus of activity shifted to more internal structures shortly after its initiation. This suggests a short-lived transition of the thrust wedge to an overcritical state, permitting rapid frontal accretion, followed by a return to (sub)critical conditions and internal shortening. The most likely cause for such an event is a transient reduction in basal strength, probably resulting from increased pore fluid pressure associated with burial of the detachment under the load of the prograding clastic wedge. The transient nature of the La Vertiente front is illustrated by the fact that it was bypassed with no sign of reactivation when thrust-front propagation toward the foreland resumed (Fig. 6). An overcritical state of the thrust wedge could also be explained by overall outward tilting of the thrust belt, as would be expected from the proposed rapid rise of the adjacent Altiplano plateau in the orogen interior (e.g., Garzione et al., 2006; Gosh et al., 2006). In such a scenario, the overcritical state would be the result of the decrease in basal dip and increase in surface slope. However, the short duration of the overcritical phase and the direct transition to an under-critical state argue against such an interpretation.

Acknowledgements

The work presented here was supported by the German Science Foundation (DFG) grant UB 61/2-1 to C.E. Uba. We thank S. Tawackoli of La Paz, David Tufino Bánzer of YPFB, and Chaco S.A., all of Santa Cruz, Bolivia, for logistical support and for providing the seismic lines used in this study. B. Fabian helped with graphic work. We thank an anonymous reviewer and particularly P. DeCelles for his very careful and thoughtful review. The ion microprobe facility at UCLA is partly supported by a grant from the Instrumentation and Facilities Program, Division of Earth Sciences, U.S. National Science Foundation.

Appendix A. Supplementary data

Supplementary data associated with this article can be found, in the online version, at doi:10.1016/j.epsl.2009.02.010.

References

Baby, P., Hérail, G., Salinas, R., Sempere, T., 1992. Geometry and kinematic evolution of passive roof duplexes deduced from cross-section balancing: example from the foreland thrust system of the southern Bolivian Subandean Zone. Tectonics 11, 523–536.

Baby, P., Rochat, P., Mascle, G., Hérail, G., 1997. Neogene shortening contribution to crustal thickening in the back-arc of the Central Andes. Geology 25, 883–886.

Barke, R., Lamb, S., 2006. Late Cenozoic uplift of the Eastern Cordillera, Bolivian Andes. Earth Planet. Sci. Lett. 249, 350–367.

Barnes, J.B., Ehlers, T.A., McQuarrie, N., O'Sullivan, P.B., Pelletier, J.D., 2006. Eocene to recent variations in erosion across the central Andean fold-thrust belt, northern Bolivia: implications for plateau evolution. Earth Planet. Sci. Lett. 248, 118–133.

Coudert, L., Frappa, M., Viguier, C., Arias, R., 1995. Tectonic subsidence and crustal flexure in the Neogene Chaco Basin of Bolivia. Tectonophysics 243, 277–292.

Cederbom, C.E., Sinclair, H.D., Schlunegger, F., Rahn, M.K., 2004. Climate-induced rebound and exhumation of the European Alps. Geology 32, 709–712.

DeCelles, P.G., Mitra, G., 1995. History of the Sevier orogenic wedge in terms of critical taper models, northeast Utah and southwest Wyoming.Geol. Soc. Am. Bull. 107, 454–462.

DeCelles, P.G., DeCelles, P.C., 2001. Rates of shortening, propagation, underthrusting, and flexural wave migration in continental orogenic systems. Geology. 29, 135–138.

DeCelles, P.G., Horton, B.K., 2003. Early to Middle Tertiary foreland basin development and the history of Andean crustal shortening in Bolivia. Geol. Soc. Am. Bull. 115, 58–77.

Dunn, J.F., Hartshorn, K.G., Hartshorn, P.W., 1995. Structural styles and hydrocarbon potential of the Subandean thrust belt of Southern Bolivia. In: Tankard, A.J., Suarez Soruco, R., Welsink, H.J. (Eds.), Petroleum Basins of South America. AAPG Mem., vol. 62, pp. 523–543.

Echavarria, L., Hernández, R., Allmendinger, R., Reynolds, J., 2003. Subandean thrust and fold belt of northwestern Argentina: geometry and timing of the Andean evolution. AAPG Bull. 87, 965–985.

Ege, H., 2004. Exhumations- und Hebungsgeschichte der zentralen Anden in Südbolivien (21°S) durch Spaltspur-Thermochronologie an Apatit. Ph. D. Thesis, Freie Universität Berlin, Berlin.

Ege, H., Sobel, E.R., Scheuber, E., Jacobshagen, V., 2007. Exhumation history of the southern Altiplano plateau (southern Bolivia) constrained by apatite fission track thermochronology. Tectonics 26. doi:10.1029/2005TC001869.

Flemings, P.B., Jordan, T.E., 1990. Stratigraphic modeling of foreland basins: interpreting thrust deformation and lithosphere rheology. Geology 18, 343–430.

Garzione, C.N., Molnar, P., Libarkin, J.C., MacFadden, B.J., 2006. Rapid late Miocene rise of the Bolivian Altiplano: evidence for removal of mantle lithosphere. Earth Planet. Sci. Lett. 241, 543–556.

Ghosh, P., Garzione, C.N., Eiler, J.M., 2006. Rapid uplift of the Altiplano revealed through ^{13}C–^{18}O bonds in Paleosol carbonates. Science 311, 511–515.

Graham, A., Gregory-Wodzicki, K.M., Wright, K.L., 2001. Studies in neotropical paleobotany. XV. A Mio-Pliocene palynoflora from the Eastern Cordillera, Bolivia: implications for the uplift history of the Central Andes. Am. J. Bot. 146, 813–826.

Gubbels, T.L., Isacks, B.L., Farrar, E., 1993. High-level surface, plateau uplift, and foreland development, Bolivian central Andes. Geology 21, 695–698.

Horton, B.K., 1998. Sediment accumulation on top of the Andean orogenic wedge: Oligocene to late Miocene basins of the Eastern Cordillera, southern Bolivia. Geol. Soc. Am. Bull. 110, 1174–1192.

Horton, B.K., 2005. Revised deformation history of the central Andes: inferences from Cenozoic foredeep and intermontane basins of the Eastern Cordillera, Bolivia. Tectonics 24, 3011. doi:10.1029/2003TC001619.

Horton, B.K., DeCelles, P.G., 1997. The modern foreland basin system adjacent to the Central Andes. Geology 25, 895–898.

Hubbard, R.J., Pape, J., Roberts, D.G., 1985. Depositional sequence mapping as a technique to establish tectonic and stratigraphic framework and evaluate hydrocarbon potential on a passive continental margin. In: Berg, O.R., Woolverton, D. (Eds.), Seismic Stratigraphy II: an Integrated Approach to Hydrocarbon Exploration. AAPG Mem., vol. 39, pp. 79–91.

Hulka, C., 2005. Sedimentary and tectonic evolution of the Cenozoic Chaco foreland basin, southern Bolivia. PhD Thesis, Freie Universität Berlin, Berlin.

Huyghe, P., Galy, A., Mugnier, J.-L., France-Lanord, C., 2001. Propagation of thrust system and erosion in the Lesser Himalaya: geochemical and sedimentological evidence. Geology 29, 1007–1010.

Isacks, B.L., 1988. Uplift of the central Andean plateau and bending of the Bolivian orocline. J. Geophys. Res. 93, 3211–3231.

Kleinert, K., Strecker, M.R., 2001. Climate change in response to orographic barrier uplift: paleosol and stable isotope evidence from the late Neogene Santa Maria basin, northwestern Argentina. Geol. Soc. Amer. Bull. 113, 728–742.

Kley, J., Gangui, A.H., Krüger, D., 1996. Basement-involved blind thrusting in the eastern Cordillera Oriental, southern Bolivia: evidence from cross-sectional balancing, gravimetric and magnetotelluric data. Tectonophysics 259, 171–184.

Kley, J., Müller, J., Tawackoli, S., Jacorbshagen, V., Manutsoglu, E., 1997. Pre-Andean and Andean-Age deformation in the Eastern Cordillera of Southern Bolivia. J. S. Am. Earth Sci. 10, 1–19.

Kley, J., Monaldi, C.R., Salfity, J.A., 1999. Along-strike segmentation of the Andean foreland: causes and consequences. Tectonophysics 301, 75–94.

Marshall, L.G., Sempere, T., 1991. The Eocene to Pleistocene vertebrates of Bolivia and their stratigraphic context: a review. In: Suarez-Soruco, R. (Ed.), Fosiles y facies de Bolivia, Vertebrados. Rev. Téc. Yac. Petrol. Fis. Bolivia, vol. 1, pp. 631–652.

Marshall, L.G., Sempere, T., Gayet, M., 1993. The Petaca (late Oligocene–middle Miocene) and Yecua (late Miocene) formations of the Subandean-Chaco basin, Bolivia, and their tectonic significance. Doc. Lab. Géol. Lyon 125, 291–301.

McQuarrie, N., Horton, B.K., Zandt, G., Beck, S., DeCelles, P.G., 2005. Lithospheric evolution of the Andean fold-thrust belt, Bolivia, and the origin of the central Andean plateau. Tectonophysics 399, 15–37.

Mitchum Jr., R.M., Vail, P.R., Sangree, J.B., 1977. Seismic stratigraphy and global changes of sea level, part 6: stratigraphic interpretation of seismic reflection patterns in depositional sequences. In: Payton, C.E. (Ed.), Seismic Stratigraph; Application to Hydrocarbon Exploration. AAPG Mem., vol. 26, pp. 117–134.

Moretti, I., Baby, P., Mendez, E., Zubieta, D., 1996. Hydrocarbon generation in relation to thrusting in the Subandean zone from 18° to 22°S, South Bolivia. Pet. Geosci. 2, 17–28.

Schmitt, A.K., Lindsay, J.M., de Silva, S.L., Trumbull, R.B., 2002. In-situ U–Pb zircon ages of compositionally contrasting ignimbrites from La Pacana, North Chile: implications for the formation of stratified magma chambers. J. Volcanol. Geotherm. Res. 120, 43–53.

Schlunegger, F., Simpson, G., 2002. Possible erosional control on lateral growth of the European Central Alps. Geology 30, 907–910.

Sempere, T., Hérail, G., Oller, J., Bonhomme, M.G., 1990. Late Oligocene–early Miocene major tectonic crisis and related basins in Bolivia. Geology 18, 946–949.

Starck, D., Anzótegui, L.M., 2001. The late Miocene climate change— persistence of climate signal through the orogenic stratigraphic record in northwestern Argentina. J. S. Am. Earth Sci. 14, 763–774.

Strecker, M.R., Mulch, A., Uba, C.E., Schmitt, A.K., Chamberlain, C., 2006. Late Miocene onset of the South American Monsoon. EOS Trans. Am. Geophys. Union 87 (52) T31E-06.

Strecker, M.R., Alonso, R.N., Bookhagen, B., Carrapa, B., Hilley, G.E., Sobel, E.R., Trauth, M.H., 2007. Tectonics and climate of the southern central Andes. Ann. Rev. Earth Planet. Sci. 35, 747–787.
Uba, C.E., Heubeck, C., Hulka, C., 2005. Facies analysis and basin architecture of the Neogene Subandean synorogenic wedge, southern Bolivia. Sediment. Geol. 180, 91–123.
Uba, C.E., Heubeck, C., Hulka, C., 2006. Evolution of the late Cenozoic Chaco foreland basin, Southern Bolivia. Basin Res. 18, 145–170.
Uba, C.E., Strecker, M.R., Schmitt, A.K., 2007. Increased sediment accumulation rates and climatic forcing in the central Andes during the late Miocene. Geology 35, 979–982.
Watts, A.B., 2001. Isostasy and Flexure of the Lithosphere. Cambridge University Press, Cambridge, p. 458.
Whipple, R.X., Meade, B.J., 2006. Orogen response to changes in climatic and tectonic forcing. Earth Planet. Sci. Lett. 243, 218–228.
Willett, S.D., 1999. Orogeny and orography: the effects of erosion on the structure of mountain belts. J. Geophys. Res. 104, 28957–28965.